https://doi.org/10.22226/2410-3535-2022-3-177-183

The effect of testing conditions on stress corrosion cracking of biodegradable magnesium alloy ZK60

E. D. Merson[†,1], V. A. Poluyanov[1], P. N. Myagkikh[1], D. L. Merson[1], A. Yu. Vinogradov[2]

[†]Mersoned@gmail.com

[1]Institute of Advanced Technologies, Togliatti State University, Togliatti, 445667, Russia
[2]Department of Mechanical and Industrial Engineering, Norwegian University of Science and Technology — NTNU, Trondheim, N-7491, Norway

The effect of the chemical composition, temperature, circulation and pH of the simulated body fluid (SBF) on the corrosion and stress corrosion cracking (SCC) susceptibility of the alloy ZK60 was studied through the immersion and slow-strain rate tensile (SSRT) testing respectively. It is found that both the corrosion and SCC susceptibility of the alloy is significantly affected by chemical composition and adjustment of pH level of SBF, while the temperature and circulation of the SBF exert a minor effect on these characteristics. The pH adjustment of 0.9% NaCl solution to 7 ± 0.2 was done automatically and continuously during the SSRT testing by refreshment of the SBF. The control over pH decreased the corrosion rate and increased the SCC susceptibility of the ZK60 alloy. It is established that, in the considered SBFs (0.9% NaCl, Ringer's and Hank's solutions), the alloy ZK60 possesses the highest SCC susceptibility and the least corrosion rate in Hank's solution, while in Ringer's solution, the SCC susceptibility and corrosion resistance are lowest. It is concluded that the experimental factors considered in the present study have to be accounted for in the reliable assessment of the corrosion and SCC resistance of the biomedical Mg alloys.

Keywords: biodegradable magnesium alloys, stress corrosion cracking, slow-strain rate tensile testing, pH level adjustment, simulated body fluid.

1. Introduction

Magnesium alloys are considered as promising materials for biodegradable implants [1]. Due to their excellent biocompatibility and relatively low corrosion resistance, Mg-based alloys can completely dissolute within the human body for a reasonable time without any harmful effect. The key benefit of using the Mg biodegradable implants instead of conventional insoluble ones made of Ti or stainless steel is that the second surgery invasion associated with the extraction of the temporary implants after the healing can be avoided. To succeed in the recovery of the patient after implantation as well as to prevent the additional injury the structural integrity and the constructional strength of the implants should be maintained throughout the whole period of the healing process. Being exposed to human fluids, an implant experiences continuous corrosion damage coupled with notable mechanical loads [2]. Such service conditions are known to cause stress-corrosion cracking (SCC) in many alloys, including Mg ones [3 – 5]. Thus, besides the overload fracture caused by the too fast reduction of the cross-section under the simple anodic dissolution, the load-bearing Mg implants are at risk of brittle failure, which might occur due to SCC much before the significant corrosion damage takes place. Due to the particular danger of such sudden premature failures, the improving SCC resistance of the Mg implants is of great importance. The slow strain rate tensile (SSRT) testing has been widely used to assess the SCC susceptibility of Mg alloys in various corrosive media [3, 6, 7]. The most common way to conduct experiments of this kind is to perform tensile testing at strain rates ranging from 10^{-7} to 10^{-5} s^{-1} in non-circulating corrosive media at room temperature until fracture of the specimen [5, 8]. However, in an attempt to precisely simulate the service conditions of the medical implants, this method was modified by many researchers for the assessment of SCC resistance of biodegradable Mg alloys [9 – 12]. The alloys of this kind are usually SSRT tested in simulated body fluids (SBF) of various chemical compositions ranging from standard physiological 0.9% NaCl, Hank's and Ringer's solutions to the more complex environments simulating blood plasma referred to as modified-SBF [11,12]. The temperature of the SBF is commonly maintained in the range of 36 – 37°C [9,10,13]. Furthermore, the circulation, as well as the manual or automatic correction of the pH level of the corrosive solution, were implemented by some researchers [13]. Nevertheless, the effect of all of these methodological factors on the results of the SCC testing have not been addressed as yet. Thereby to clarify this issue, in the present paper, the effect of chemical composition, temperature, circulation and pH correction of the simulated body fluid on SCC susceptibility of the biodegradable alloy ZK60 was investigated.

2. Experimental

2.1. Materials and specimens

For the SSRT testing, the round-shaped threaded specimens with the gauge part of 30 mm length and 6 mm diameter were machined from the hot-extruded bar of commercial alloy ZK60, the chemical composition of which is provided in Table 1. The small cylindrical samples of 10 mm length and 10 mm diameter were machined from the same alloy for the immersion tests aiming at the evaluation of corrosion rate. All specimens and samples were annealed in air at 200°C for 24 h to remove any possible residual stress after fabrication.

2.2. SSRT tests

The SSRT testing in different conditions summarized in Table 2 was performed at $5 \cdot 10^{-6}$ s^{-1} strain rate using screw-driven frame AG-X Plus (Shimadzu). In accordance with Table 2 the experiments were conducted at 25 or 37°C in four different environments, including air, 0.9% NaCl, Ringer's and Hank's solutions optionally subjected to circulation and adjustment of the pH level. The chemical compositions of these standard SBF solutions are represented in Table 3. The conditions of the experiments were chosen in such a way that the effect of each experimental factor could be distinguished. The schematics of the experimental setup which was used for the SCC experiments is represented in Fig. 1. The plexiglass corrosion cell filled with corrosion solution was mounted on the specimen during the tensile testing, such that the only gauge part was contacting with the corrosion solution. The temperature control of the corrosion solution was conducted in two different ways. At the experimental conditions #2 and 3, the corrosion solution was not circulated, while its temperature was maintained at 25 or 37 ± 0.2°C by the use of the heat exchanger, which is represented by the water-

Table 2. The experimental conditions used for the SSRT tests.

#	Environment	Temperature, °C	Circulation	pH adjustment
1	Air	25	-	-
2	0.9% NaCl	25	-	-
3	0.9% NaCl	37	-	-
4	0.9% NaCl	37	+	-
5	0.9% NaCl	37	+	+
6	Ringer's	37	+	+
7	Hank's	37	+	+

Table 3. The chemical composition of the SBFs used in the SSRT and immersion tests, g/l.

Component	0.9% NaCl	Ringer's	Hank's
NaCl	9	8.6	8
$CaCl_2$	-	0.25	0.14
KCl	-	0.3	0.4
KH_2PO_4	-	-	0.06
$MgCl_2 \cdot 6H_2O$	-	-	0.1
$MgSO_4 \cdot 7H_2O$	-	-	0.06
$Na_2HPO_4 \cdot 12H_2O$	-	-	0.48
$NaHCO_3$	-	-	0.35
D-glucose	-	-	1

Table 1. Chemical composition of the alloy ZK60 (in wt.%).

Mg	Al	Zn	Ca	Zr	Fe	Cu	Mn	Ce	Nd	Si
Balance	0.002	5.417	0.0004	0.471	0.001	0.002	0.005	0.002	0.003	0.003

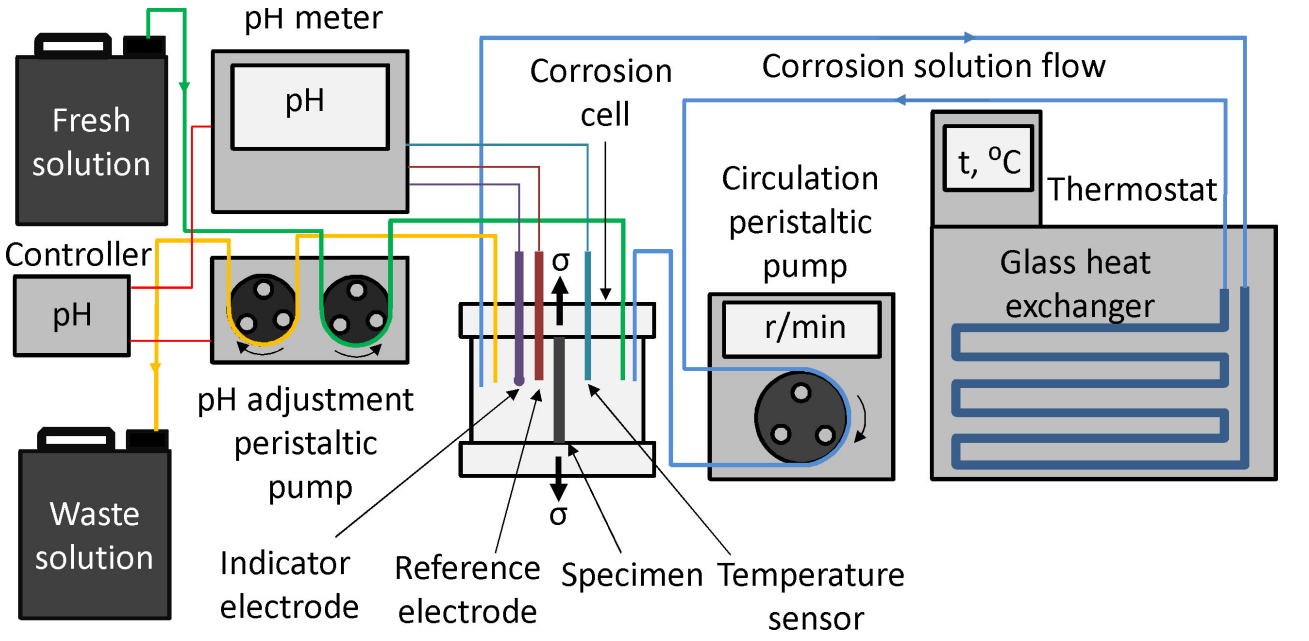

Fig. 1. (Color online) The schematics of the experimental setup allowing temperature control, circulation and pH level adjustment of the corrosion solution contacting with the gauge part of the specimen subjected to slow strain rate tensile testing.

coolant glass coil-pipe twined around the specimen's gauge part. In this case, the coolant was circulated within the heat exchanger, thermostat and silicone pipes by the peristaltic pump. In experiments #4 – 7, the corrosion solution itself was circulated by the peristaltic pump through the tract, including the corrosion cell, the system of the silicone pipes and the glass coil-pipe submerged into the water tank of the thermostat. In the experiments #5 – 7, during the whole tensile testing, the pH level of the corrosion solution inside the corrosion cell was automatically adjusted at 7.0 ± 0.2 value by the simultaneous pumping in of the fresh corrosion solution and pumping out of the waste one by the two-rotor peristaltic pump which was triggered by the signal from pH-meter. The schematics represented in Fig. 1 illustrates the experimental setup for conditions #5 – 7. The experiments with the Ringer's and Hank's solutions (#6 and 7) were conducted at 37°C with circulation and pH adjustment of the corrosion solution. All the experiments under specific experimental conditions were duplicated to assess the reproducibility.

2.3. Microscopy

After the specimens were fractured during the tensile testing, they were rapidly extracted from the corrosion cell, rinsed with ethanol and dried by compressed air to minimize the additional corrosion damage of the fracture surfaces. The fractographic examination was conducted by the scanning electron microscope JCM-6000 (JEOL).

2.4. Immersion tests

To study the relationship between the regular corrosion and the results of the SSRT testing, the corrosion rate of the small samples of the same alloy was evaluated by the gravimetric method during the immersion tests. The experimental conditions during these tests were similar to those used for the SSRT testing and are represented in Table 2. The only difference from the SSRT tests was in that the temperature maintenance both at 25 and 37°C in the immersion tests was performed only by the circulation of the corrosion solution. During the test, the samples were placed inside the glass beaker filled with the corrosion solution. The circulation and pH correction of the corrosion solution during the immersion tests were performed in the same way to that in the SSRT tests as is described above. The duration of all immersion tests was 24 h. After the finishing of the test, the samples were extracted from the corrosion solution, rinsed with ethanol, dried by compressed air and then subjected to removal of corrosion products through their submerging for 1 min into the standard 20% CrO_3 +1% $AgNO_3$ aqueous solution followed by weighting. The corrosion rate was calculated by the standard weight-loss method.

3. Results

3.1. Immersion testing

The immersion testing showed that the alloy ZK60 demonstrates almost the same corrosion rate at 25 and 37°C in the circulated 0.9% NaCl, see Fig. 2 a. The use of pH adjustment resulted in a notable decrease in corrosion rate. At all other equal conditions (37°C, circulation and pH correction) the highest corrosion rate is observed in Ringer's solution, while the lowest corrosion rate corresponds to Hank's solution.

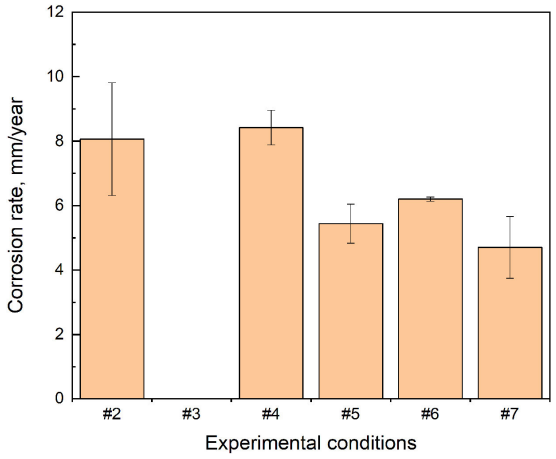

a

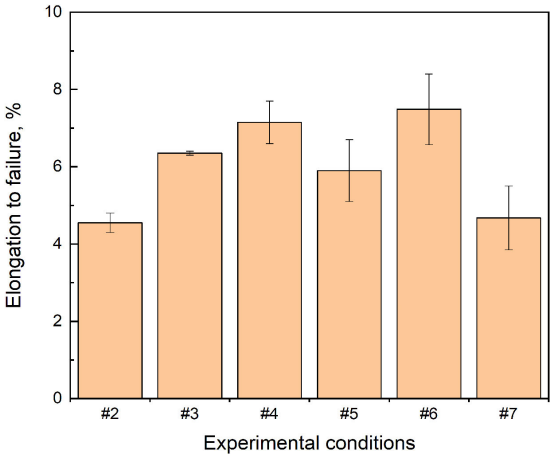

b

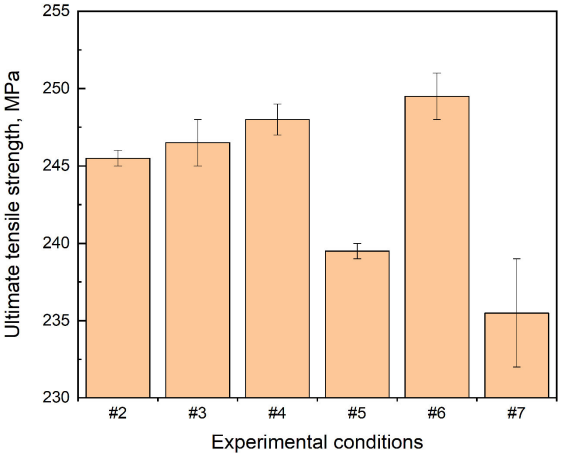

c

Fig. 2. The effect of the experimental conditions specified in Table 2 on corrosion rate (a), elongation to failure (b) and ultimate tensile strength (c) of the alloy ZK60 subjected to immersion (a) and SSRT (b, c) testing.

3.2. SSRT testing

The results of mechanical testing showed that all the specimens which were tested in the SBFs (#2-7) suffer SCC, as is indicated by the substantial reduction of both the ultimate tensile strength (UTS) and elongation to failure (EF) with respect to the specimens tested in air (#1), see Fig. 2 b, c and 3. However, it should be noted that the specimens tested in SBF at all conditions break at the stress fairly higher than the yield strength and demonstrate slight elongation before fracture. The degree of ductility and strength loss due to SCC depends on the experimental conditions of the SSRT testing. As follows from Fig. 2 b, c, UTS of the specimens tested in 0.9% NaCl solution is almost not dependent on temperature, whereas their EF at 25°C (#2) is notably lower than at 37°C regardless of whether the corrosion solution was circulated (#4) or not (#3). Nevertheless, the mechanical properties of the specimens tested in the circulating SBF demonstrate slightly less degradation of mechanical properties due to SCC in comparison with the specimens tested in the stagnant solution of the same chemical composition and temperature. It is found that pH of the corrosion solution in the corrosion cell increases rapidly after the beginning of tensile testing (unless pH is not corrected externally) and saturates at 9.8 – 10.2 after about 40 minutes of the experiment, as is illustrated by the pH curves #2 – 4 in Fig. 4. The system of pH correction allows maintaining the pH level at 7 ± 0.2, as is evidenced by the oscillating curve #5 in Fig. 4. Such the correction of pH level exerts a significant effect on the SCC susceptibility as is evidenced by the substantial drop of UTS and moderate decrease of EF. The SSRT tests, which were conducted in different SBFs at 37°C with circulation and pH correction of the corrosion solution, showed that the most severe SCC occurs in Hank's solution, while the Ringer's one produces the least effect on the mechanical response of the alloy.

3.3. Fractography

The fractographic study showed that all specimens tested in 0.9% NaCl or Ringer's solutions have almost completely brittle fracture surfaces, which are featured by pronounced crack nucleation sites as is indicated by the fan-like patterns originating at the specimens' side surface, see Fig. 5 a. It can be seen at a higher magnification that the nucleation of the cracks in 0.9% NaCl and Ringer's solutions occurred at fairly deep corrosion pits on the side surface of the specimens, Fig. 5 b. Once nucleated, the cracks propagate towards the specimens' centre. All the fracture surfaces obtained in 0.9% NaCl and Ringer's solution are similar in terms of the fraction of brittle components, morphology and other features; thus, the effect of temperature, circulation and pH correction of the corrosion solution on the fracture surface of the specimens is concluded to be minor. Interestingly, the fracture surfaces of the specimens which were tested in Hank's solution are contrasting with the other ones. Firstly, these fracture surfaces have a fairly large area of the ductile dimpled relief, which was obviously formed during the final fracture, e. g. Fig. 5 c. Secondly, it can be seen from Fig. 5 c and d, that, in contrast to those of the specimens tested in other SBFs, the fracture surface of the specimens tested in Hank's solution exhibit neither clearly visible nucleation points of the cracks nor the corrosion pits such as those shown in Fig. 5 b. Apparently, the cracks in Hank's solution nucleated at numerous multiple points along the whole side surface and propagated towards the centre of the specimen. The morphology of the fracture surface in all solutions was represented by cleavage, intergranular and fluted facets. The features of these typical fracture surface morphologies of the ZK60 alloy subjected to SCC have been considered in detail elsewhere [5,14].

4. Discussion

The results of the present study show that the most pronounced effect on the degree of SCC of ZK60 alloy is produced by the temperature, pH correction and chemical composition of the SBF, while the circulation of the solution exerts minor influence. Among the investigated SBFs, Hank's solution causes the most severe SCC and, at the same time, the least corrosion rate. On the other hand, Ringer's solution produces the least effect on mechanical properties but causes the highest corrosion rate. Thus, the obtained results suggest that, at all other conditions being equal, the SCC susceptibility of the alloy ZK60 is higher in the SBFs, causing a lower corrosion rate. A similar relationship between the SCC susceptibility and corrosion rate can be traced from experiments #4 and 5. It is shown in these tests that the pH correction of the 0.9% NaCl solution results in an increase in the SCC susceptibility, but it decreases the corrosion rate of the alloy. In this context, the effect of temperature seems to be in contrast with the other results. It is established that an increase in temperature of the corrosion solution almost does not affect the corrosion rate but results in the significant decrease of ductility loss induced by SCC. However, it is worth noting that the UTS values of the specimens, which were tested at 25 and 37°C, are very close to each other, Fig. 2 c. On the other hand, one can notice, Fig. 3, that the stress-strain curve of the specimen tested in 0.9% NaCl at

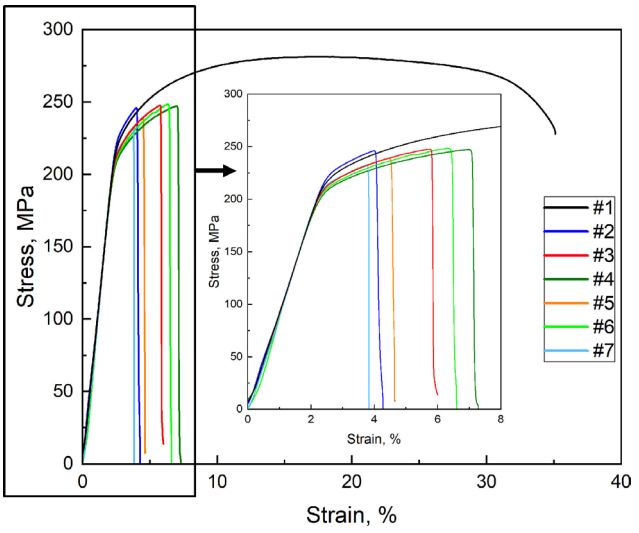

Fig. 3. (Color online) The effect of the experimental conditions specified in Table 2 on stress-strain diagrams recorded during SSRT testing of the specimens of the alloy ZK60.

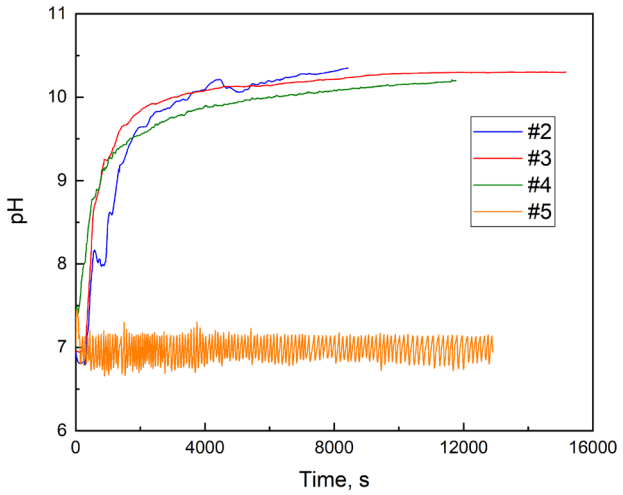

Fig. 4. (Color online) The evolution of pH throughout the SSRT test of the specimens of the alloy ZK60 at different experimental conditions specified in Table 2.

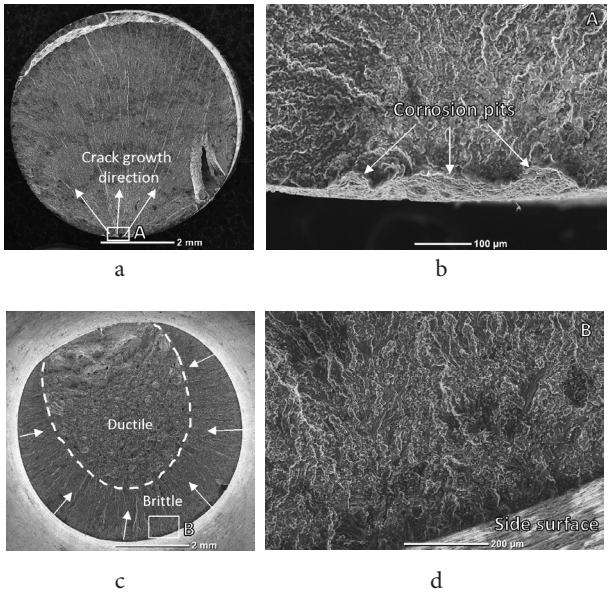

Fig. 5. Fractographic features of the specimens of the alloy ZK60 SSRT tested in the Ringer's (a, b) and Hank's (c, d) solutions: the full views of the fracture surface (a, c), the magnified areas outlined by the frames "A" and "B" in (a) and (c) respectively (b, d).

25°C superimposes with that of the specimens tested in air at the same temperature. In contrast, all the stress-strain curves, which were obtained at 37°C, lie below the curves obtained at 25°C and are fairly well superimposed on each other regardless of the experimental conditions. Thus, it is apparent from the obtained results that the strain-hardening behaviour of the present alloy significantly depends on temperature but is just slightly affected by the other experimental conditions considered in the present study. Recently it was shown that the alloy used in the present study possesses extremely high strain-rate sensitivity [15], hence, indicating the pronounced thermally-activated nature of the mechanism governing the plastic deformation in this alloy. Thus, such a strong effect of even a slight change in the temperature on strain-hardening behaviour observed in the present work is not surprising. It can be suggested that fracture of the specimens due to SCC occurs at certain critical threshold stress, which depends on corrosion resistance of the alloy at specific experimental conditions. The existence of such threshold stress triggering SCC in Mg alloys has been suggested and discussed by many researchers [4,16]. In accordance with the suggestion made, the comparable level of UTS of the specimens tested at 25 and 37°C are well expected because the corrosion rates of these specimens are almost the same. However, due to the different strain-hardening behaviour of the considered specimens, which is apparently caused by the different temperatures of the corrosion solution, the same UTS is reached at different elongations. This can explain the greater ductility loss recorded for the specimens tested at room temperature in comparison to those tested at 37°C. Since all the specimens tested at 37°C demonstrate similar strain-hardening behaviour, both the ductility and strength loss of these specimens due to SCC are equally affected by the experimental conditions.

For the explanation of the observed results the mechanisms of corrosion of Mg in aqueous solutions are to be considered. It is generally accepted that the corrosion process includes the following reactions [17]:

$$2H^+ + 2e = H_2\uparrow \quad \text{(cathodic partial reaction)} \qquad (1)$$

$$2Mg = 2Mg^+ + e \quad \text{(anodic partial reaction)} \qquad (2)$$

$$2Mg^+ + 2H^2O = 2Mg^{++} + 2OH^- + H_2\uparrow \quad \text{(chemical reaction)} \qquad (3)$$

$$2Mg + 2H^+ + 2H_2O = 2Mg^{++} + 2OH^- + 2H_2\uparrow \quad \text{(overall reaction)} \qquad (4)$$

$$Mg^{2+} + 2OH^- = Mg(OH)_2 \quad \text{(product formation)} \qquad (5)$$

$$Mg + 2H_2O = Mg(OH)_2 + H_2\uparrow \quad \text{(overall reaction in steady state)} \qquad (6)$$

The surface film of $Mg(OH)_2$ protects Mg from further dissolution in water. However, in presence of Cl^- anions $Mg(OH)_2$ is unstable and dissolves with formation of $MgCl_2$ and OH^-. The corrosion mechanism of Mg in Cl-containing aqueous solutions is given by [18]:

$$Mg(OH)_2 + 2Cl^- \rightarrow MgCl_2 + 2OH^- \qquad (7)$$

$MgCl_2$ is unstable in water and dissociates in accordance with reaction:

$$MgCl_2 \rightarrow Mg^{2+} + 2Cl^- \qquad (8)$$

Furthermore, the $Mg(OH)_2$ film can be raptured under external mechanical loading, for example during SSRT testing. The micro cracks producing inside the protective hydroxide layer due to such rapture as well as the corrosion pits forming due to localized anodic dissolution play the role of the stress risers and, thus, may serve as the favorable nucleation points for SCC [17]. The further propagation of the stress corrosion crack is accompanied by the repeated cycles of passivation of the newly formed surface in the crack wake, rupturing of the protective film under mechanical loading, as well as under reaction with Cl^- and anodic dissolution. It has been reported that in certain conditions, the passivation of the newly formed Mg surface in the crack tip can be as such as fast that corrosion and SCC do not occur even under continuously rising mechanical external load [17,19]. On the other hand, the too fast anodic dissolution can outrun

the propagation of the crack or can result in blunting of the crack tip. That is why it is generally accepted that maximum SCC susceptibility appears at a certain balance between the passivation and anodic dissolution reactions [17]. In accordance with fracture mechanics, the sharper the crack tip nuclei, the lower the stress required for propagation of the brittle crack. Thereby, at a high corrosion rate, the crack tip can probably blunt under the anodic dissolution, resulting in higher external threshold stress required for propagation of this crack. This can possibly explain the relationship between the corrosion rate and SCC susceptibility observed in the present study for alloy ZK60, which possesses a relatively high corrosion rate in NaCl-based solutions. It should be noted that the relationships found in the present study are fair for ZK60 alloy in the considered conditions and probably for the other alloys with relatively high corrosion rates but can be different for other alloys and corrosion solutions. Thus, the additional investigations are required to reveal the more general relationships.

The effect of testing conditions on the corrosion rate is of particular interest. It follows from the reactions considered above that the corrosion process consumes water and hydrogen ions due to the evolution of hydrogen gas, while Cl^- anions recursively transfer from the solution to $MgCl_2$ and back. Thus, the concentration of Cl^- in the solution should increase during the corrosion process until saturation. The increase in the concentration of Cl^- ions in the solution is known to accelerate the corrosion of Mg. On the other hand, the continuous formation of hydroxide protective film inhibits the corrosion process, while the increase of concentration of OH^- ions in the solution results in the increase of the pH value, as can be seen in Fig. 4. The increasing corrosion rate of many Mg alloys, including ZK60, during their immersion in various NaCl-based corrosion solutions, has been reported [20]. This can be due to the increasing Cl^- concentration in the solution. In experiments #5 – 7, pH of the solution was automatically adjusted at 7.4 by pumping-in the fresh solution with a low Cl^- concentration and pumping-out the waste with a high Cl^- concentration. Thus, this can explain the lower corrosion rate of the samples which were tested with the pH correction in comparison with those which were tested without pH correction. It is found in the present paper that the corrosion rate of ZK60 depends on the composition of the corrosion solution in the following order Ringer's > 0.9 NaCl > Hank's. The concentration of Cl^- anions in these solutions decreases in the same order: 164, 154 and 145 mmol/l for Ringer's, 0.9 NaCl and Hank's solutions, respectively. This can be the one reason for the observed relationship between corrosion rate and compositions of the SBF. Furthermore, it is known that the dual protective film composed of $Mg(OH)_2$ and the dense top layer containing CaP is formed on the Mg surface in Hank's solution [21]. This film exerts a much better protective effect against corrosion than ordinary porous hydroxide film forming in 0.9%NaCl and Ringer's solutions.

5. Conclusions

1. The chemical composition and adjustment of pH value of the simulated body fluid (SBF) exert a significant effect on the susceptibility of the biodegradable Mg alloys to stress corrosion cracking (SCC) at slow-strain rate tensile (SSRT) testing as well as to general corrosion at immersion tests. Thus, to assess the corrosion and SCC resistance of the biomedical Mg alloys, the aforementioned experimental factors have to be accounted for and adjusted to simulate the actual service conditions of the alloys.

2. The adjustment of the 7 ± 0.2 pH level of 0.9% NaCl solution during the SSRT testing by automatic refreshment of the SBF decreases the corrosion rate and increases SCC susceptibility of the ZK60 alloy.

3. In the considered SBFs (0.9% NaCl, Ringer's and Hank's solutions), the alloy ZK60 possesses the highest SCC susceptibility and the least corrosion rate in Hank's solution, while in Ringer's solution, the SCC susceptibility and corrosion resistance of this alloy are smallest.

4. The temperature and circulation of the SBF exert a minor effect on the SCC susceptibility of ZK60 alloy in terms of threshold stress of SCC. However, the change in temperature of the testing environment from 25 to 37°C can affect the strain-hardening behaviour of the ZK60 alloy, thus, causing the apparent ductility loss during the SSRT testing in corrosive media.

Acknowledgements. Financial support from the Russian Science Foundation through the grant-in-aid No. 21-79-10378 is gratefully appreciated.

References

1. Y. Chen, J. Dou, H. Yu, C. Chen. J. Biomater. Appl. 33, 1348 (2019). Crossref
2. X. Li, C. Chu, P.K. Chu. Bioact. Mater. 1, 77 (2016). Crossref
3. S. Jafari, S.E. Harandi, R.K. Singh Raman. Jom. 67, 1143 (2015). Crossref
4. A. Atrens, N. Winzer, W. Dietzel. Adv. Eng. Mater. 13, 11 (2011). Crossref
5. E. Merson, V. Poluyanov, P. Myagkikh, D. Merson, A. Vinogradov. Acta Mater. 205, 116570 (2021). Crossref
6. F. Qi, X. Zhang, G. Wu, W. Liu, L. Wen, H. Xie, S. Xu, X. Tong. Mater. Charact. 183, 111630 (2022). Crossref
7. E. Merson, V. Poluyanov, P. Myagkikh, D. Merson, A. Vinogradov. Mater. Sci. Eng. A. 806, 140876 (2021). Crossref
8. L. He, J. Yang, Y. Xiong, R. Song. Mater. Chem. Phys. 261, 124232 (2021). Crossref
9. J. Jiang, Q. Xie, M. Qiang, A. Ma, E.K. Taylor, Y. Li, D. Song, J. Chen. J. Rare Earths. 37, 88 (2019). Crossref
10. S. Jafari, R.K.S. Raman, C.H.J. Davies. Eng. Fract. Mech. 201, 47 (2018). Crossref
11. L. Chen, C. Blawert, J. Yang, R. Hou, X. Wang, M.L. Zheludkevich, W. Li. Corros. Sci. 175, 108876 (2020). Crossref
12. D.B. Prabhu, J. Nampoothiri, V. Elakkiya, R. Narmadha, R. Selvakumar, R. Sivasubramanian, P. Gopalakrishnan, K.R. Ravi. Mater. Sci. Eng. C. 106, 110164 (2020). Crossref
13. B.J. Wang, D.K. Xu, J. Sun, E.H. Han. Corros. Sci. 157, 347 (2019). Crossref

14. E. Merson, V. Poluyanov, P. Myagkikh, D. Merson, A. Vinogradov. Mater. Sci. Eng. A. 772, 138744 (2020). Crossref
15. E. Merson, V. Poluyanov, P. Myagkikh, D. Merson, A. Vinogradov. Mater. Sci. Eng. A. 830, 142304 (2022). Crossref
16. W.R. Wearmouth, G.P. Dean, R.N. Parkins. CORROSION. 29, 251 (1973). Crossref
17. N. Winzer, A. Atrens, G. Song, E. Ghali, W. Dietzel, K.U. Kainer, N. Hort, C. Blawert. Adv. Eng. Mater. 7, 659 (2005). Crossref
18. M. jie Liang, C. Wu, Y. Ma, J. Wang, M. Dong, B. Dong, H. hong Liao, J. Fan, Z. Guo. Mater. Sci. Eng. C. 119, 111521 (2021). Crossref
19. K. Ebtehaj, D. Hardie, R.N. Parkins. Corros. Sci. 28, 811 (1988). Crossref
20. A. Atrens, G.L. Song, M. Liu, Z. Shi, F. Cao, M.S. Dargusch. Adv. Eng. Mater. 17, 400 (2015). Crossref
21. C. Taltavull, Z. Shi, B. Torres, J. Rams, A. Atrens, J. Mater. Sci. Mater. Med. 25, 329 (2014). Crossref